Parameters of Influence in Surface Ablation and Texturing of Metals Using High-power Ultrafast Laser

John LOPEZ[*1], Marc FAUCON[*2], Raphael DEVILLARD[*1], Yoann ZAOUTER[*3], Clemens HONNINGER[*3], Eric MOTTAY[*3] and Rainer KLING[*2]

[*1] *Univ Bordeaux, Cnrs Cea, Umr5107, 33405 Talence, France*
E-mail: lopez@celia.u-bordeaux1.fr
[*2] *Alphanov, Bât. IOA, Rue François Mitterrand, 33400 Talence, France*
[*3] *Amplitude Systemes, 11 Avenue de Canteranne, 33600 Pessac, France*

High power ultrafast lasers are nowadays able to provide high ablation rates and meet the technical requirements and performances needed for many industrial applications. However depositing more energy into the target may induce heat accumulation, and consequently enhances the ablation efficiency as well as introduces some detrimental effect on the processing quality. So, the key issue is to improve throughput while maintaining the processing quality and preventing from any deformation of the work piece. In this paper we present some comparative results on surface ablation of Aluminum, Copper, Molybdenum and stainless steel in both picosecond and femtosecond regimes. Trials have been performed using two high power Yb-doped fibre ultrafast lasers which are tunable in pulse duration (350 fs to 10 ps, up to 20 W). Samples have been characterized with confocal microscopy and scanning electron microscopy. We discuss the effect of pulse duration, repetition rate, fluence and energy dose per mm on ablation efficiency, processing quality and ripples formation.

DOI: 10.2961/jlmn.2015.01.0001
Keywords: Ablation, efficiency, pulse duration, femtosecond, picosecond, stainless steel, copper

1. Introduction

The relevance of ultrashort laser is nowadays well established for many medical or industrial applications. Indeed, the ultrashort laser technology has reached a high robustness level that is compatible with the needs of industry. This laser technology combines the unique capacity to process any type of material with an outstanding precision and a reduced heat affected zone [1-2]. Thanks to high average power and high repetition rate it is possible today to achieve high throughput [3], providing that the operating parameters are finely tuned to the application, otherwise heat accumulation and heat affected zone may appear.

In this paper we present some experimental results on single pass engraving of Stainless Steel at high repetition rates (up to 2 MHz) and high average power (up to 15 W). Several parameters of influence such as fluence, pulse duration, repetition rate, dose per millimeter and scanning velocity have been considered. Results obtained on Stainless Steel are compared to those previously obtained on Aluminum, Copper and Molybdenum [4-5]. Results will be discussed in terms of etch rate, etch rate per average power, etch rate per fluence, ablation efficiency and processing quality.

2. Parameters of influence in ultrashort pulse ablation

2.1 Ablation mechanism

The ablation mechanism with ultrashort pulses is governed by the laser properties as well as the optical and the thermo-physical properties of the material. The ultrashort ablation mechanism has been described in several key papers in the last decades [1-2,6-7]. For metals, the absorption generally occurs in free electrons of the conductive band thanks to inverse Bremsstrahlung. This absorption is followed by a fast energy relaxation and thermalization within the electronic subsystem on a femtosecond timescale, a localized heat diffusion by hot electrons, and finally an energy transfer from hot electrons to the lattice on a longer time scale, ranging from few picoseconds to few tens of picoseconds for different metals, owing to the photon-electron coupling [8].

2.2 Parameters of influence

Parameters of influence in surface ablation and their process window have been reviewed and discussed in previous papers [1-2,4-5, 9-11].

In the middle of the 90's Momma et al. have published very impressive micrographies of stainless steel drilled in the nanosecond, picosecond and femtosecond regimes, showing that ultrashort pulses enable to reduce burr and droplets in the vicinity of the hole at low repetition rate with Ti:Sa lasers [2]. Indeed, thanks to the extremely short of the pulse (below 200 fs), the thermal diffusion into the surrounding bulk material can be neglected. Lopez et al. have underlined that the effect of pulse duration is material dependent [5].

In addition, etch rate should normally increase with fluence, but Chichkov et al. have shown that, even in the femtosecond-picosecond range, near-threshold fluences (optical regime, 200 to 600 mJ/cm²) lead to a better processing quality than higher fluences (thermal regime, 600 mJ/cm² to 6 J/cm²) [1]. Furthermore, Lopez and Neuenschwander have pointed out an optimum in fluence, near

the threshold, that gives the best ablation efficiency [4-5,11].

Vorobyev et al. have shown that heat accumulation is possible in metal such as Copper or Magnesium in the femtosecond regime [12]. This observation has been done at 800nm, 1 kHz and 60 fs. With these operating conditions, heat accumulation rises above 0.1 J/cm² for Copper and 0.04 J/cm² for Magnesium. Moreover, heat accumulation enhances the etch rate, but also introduces some detrimental effects on the processing quality [4-5, 10]. The effect of heat accumulation increases at high repetition rates [10] and high fluences [1].

Furthermore, particles and plasma shielding may occur if the temporal delay between two consecutive pulses is too short with respect to the lifetime of the ablation plume. Indeed, König et al. have used a pump-probe-based time-resolved plasma attenuation experiment in order to measure the plume lifetime during laser ablation of Aluminum in the femtosecond regime (200 fs, 17 J/cm²). With their set of parameters, particles shielding occurs above 200 kHz and plasma shielding above 5 MHz [13].

Ancona et Döring have measured the number of pulses to go through a stainless steel foil with picosecond (6 and 19 ps) and femtosecond pulses (800 fs) and with repetition rates ranging from 100 kHz to 1 MHz. First of all, the femtosecond regime appears to be more efficient (less pulses are required). Secondly, in the range of 300 to 500 kHz, the heat accumulation induced by high repetition rate becomes sufficient enough to overcome the negative effect of particles shielding and to enhance the drilling rate [10]. They have also shown that the effects of heat accumulation and of particles shielding are material dependent.

3. Experimental setup and protocol

3.1 Laser source

All trials on Stainless Steel have been performed with a commercial Yb-doped fiber ultrashort pulse laser from Amplitude Systemes (model Tangerine). The operating wavelength is 1030 nm. The maximum average power is 20 Watt. The M² factor is about 1.2 (figure 1, left). The repetition rate is ranging from 200 kHz to 2 MHz. An internal pulse picker enables to generate lower repetition rates down to 1 kHz. The pulse duration can be easily tuned from 300 fs to 10 ps, but it can't go above 1ps at 200 kHz (figure 1, right). The pulse duration and the average power were measured with a Pulse Check autocorrelator and a Coherent powermeter respectively.

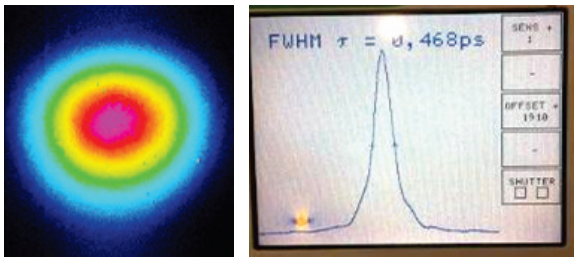

Fig. 1 Spatial (left) and temporal (right) shape of the laser beam after halfwave plate. Beam size at 1/e² is 2.92 mm on major axis and 2.64 mm on minor axis. The decorrelation factor is 1.543 so the pulse duration is here 300 fs. Rep. rate is 200 kHz.

3.2 Experimental setup

The experimental setup includes the following elements: the Tangerine laser, a halfwave plate and a polarizer cube for power tuning, a 2x-beam expander, a 2-axis galvo head (Scanlab) for beam motion on the target, a 100 mm-f(theta) focusing lens, a set of XYZ-motorized stages (Newport) for focus setting and for positioning the sample under the laser beam, and finally a sample holder. The optical transmission between the laser output and the target is about 90 ± 5 %. The average power measurement is made after the focusing lens. The spot size (at 1/e²) is measured thanks to a BeamMap2 M²-meter. The spot size is 28 ± 2 µm for all trials. The fluence is calculated by dividing the pulse energy by the spot area. The resulting fluence has been varied from 0.1 to 12 J/cm² for all trials.

3.3 Target material

Trials have been done on austenitic stainless steel AISI 316L foils with a thickness of 100 µm. These samples were provided from Goodfellow. We applied no cleaning before laser treatment.

3.4 Experimental protocol

The experimental protocol is based on a single pass process. For each set of parameters (pulse duration, repetition rate, and average power) we have produced a pattern composed by 14 parallel lines with scanning velocities ranging from 1 to 2000 mm/s. Each line produces a groove on the target. Depth and width depend on the operating parameters. The scanning velocities have been checked by measuring the distance between two subsequent spots at low repetition rate. The polarization of the laser beam is linear and perpendicular to the motion of the beam on the target. We have considered 4 levels in average power: 2, 5, 10 and 15 W. Thus, depending on the repetition rate and on the scanning velocity, we have collected data with fluences ranging from 0.2 to 13 J/cm². The pulse-to-pulse linear overlap ranges from 64 to 99.9%. So, each point of the surface has received from 6 to 1100 pulses. Uncertainty is about ±9% on fluence, ±4% on etch rate, ±9% on etch rate per average power, ±13% on etch rate per fluence and ±9% on ablation efficiency (see paragraph 4).

3.5 Comparison with previous results on Aluminum, Copper and Molybdenum

The results on Stainless Steel have been compared to those previously obtained on Aluminum, Copper and Molybdenum using a non-commercial 40W-tunable CPA Yb-doped fiber ultrashort pulse laser made by Amplitude Systemes and an optical setup similar to the one used in the present work [5].

3.6 Samples characterization

The profile of each groove (depth and width) was measured using a Leica DCM 3D confocal microscope based on LED technology with a 100x/0.90-objective. Each depth measurement is the mean of five measurements. The width was ranging from 10 to 34 µm, depending on the pulse duration, the scanning velocity and the average power. The most significant measurements were obtained on

grooves with depth between 0.3 to 22 µm, and with aspect ratio below 1. For groove with aspect ratio above 1, the roughness and the shape of sidewalls induce light trapping and shadowing effects which reduce the accuracy of the measurement. Furthermore, below 0.3 µm the groove is not deep enough, compared to the initial sample roughness, to get a significant depth measurement. Since each groove has a triangular-like cross-section area, the etch rate per pulse or per minute is calculated from the cross-section area, the scanning velocity and the repetition rate.

Scanning electronic microscopy (SEM) analyses were also performed using a Phenom ProX microscope in order to observe the processing quality in the vicinity of the grooves. This SEM microscope offers two modes: the full mode which gives a realistic view of the surface and the topography mode which is more suitable to enhance high and low-relief. The samples have been cleaned in an ultrasonic bath (3 min, water, 30°C) before SEM analysis.

4. Characteristics of interest

Several physical characteristics have been considered in order to analyze the influence of each parameter on the single pass engraving process.

4.1 Etch rate and removal rate

We define etch rate as the ablated volume per pulse [$\mu m^3 \cdot pls^{-1}$], and the removal rate as the ablated volume per minute [$mm^3 \cdot min^{-1}$]. Since we have tried several scanning velocities, ranging from 1 to 2000 mm/s, we may have several operating points for each set of parameters (pulse duration, repetition rate and average power). We assume that the optimum scanning velocity may change with other operating parameters. So we will only keep the operating point leading to the highest etch rate or removal rate, which is called the best operating point. This protocol has been described in details a previous paper [5].

4.2 Etch rate per fluence and etch rate per average power

From an efficiency point of view, is it more relevant for a given pulse energy to use a small spot with high fluence or a large spot with a low fluence? What is the maximum amount of material that can be removed per watt? To answer these questions we introduce etch rate per fluence [$\mu m^3 \cdot pls^{-1} \cdot J^{-1} \cdot cm^2$] and removal rate per average power [$mm^3 \cdot min^{-1} \cdot W^{-1}$]. The two characteristics are complementary since the first one describe the efficiency of a unique pulse meanwhile the second one takes into account the effect of repetition rate. Several authors have recently pointed out an optimum in fluence near the ablation threshold that gives the best etch rate per fluence [5] or removal rate per average power [14-16]. Neuenschwander et al. have proposed a model to explain this tendency [14-16]. The optimum in fluence F_{opt} is defined as $e^2/2$ times the threshold fluence. This optimum in fluence is shifted to lower fluences when the pulse duration decreases [14].

The maximum value in etch rate per fluence or in removal rate per average power, which is related to the process efficiency, can be plotted as a function of fluence, repetition rate, pulse duration energy or dose per millimeter as shown in chapter 5.

4.3 Ablation efficiency

From our experiments we can calculate the energy required to remove 1 mm^3 of metal, which is called E_{exp}. The unit is [$J \cdot mm^{-3}$]. The calculation is based on the formula $E_{th}=P/(V*S)$, where P is the average power [W], V the scanning velocity [$mm \cdot s^{-1}$] and S the cross section of the groove [mm^2].

From a theoretical point of view, it is possible to calculate the minimum value of energy that is needed to bring 1 mm^3 of metal just above its boiling temperature and to evaporate it. This energy, called E_{th}, can be calculated on the basis of thermo dynamical laws, by adding melting enthalpy (δH_{melt}), boiling enthalpy (δH_{boil}) and the enthalpy required to heat the metal from ambient temperature to a temperature just above its boiling temperature (δH). This latter enthalpy has been calculated using the Shomate equation for all metal but for alloy [17]. So, theoretical data for 316L Stainless are estimated using the composition of the alloy, about 69% Fe, 17% Cr, 12% Ni and 2% Mo. All data are regrouped in table 1.

Table 1 Theoretical calculation of energy required to vaporize 1 mm3 of metal

Material	δH J/mm³	δH_{melt} J/mm³	δH_{boil} J/mm³	E_{th} J/mm³
Stainless Steel	18.4	2.2	59.6	80
Aluminum	8.0	1.1	34.0	43,1
Copper	12.9	1.7	47.6	62.2
Molybdenum	21.6	4.5	70.6	96.7
Iron	18.8	1.7	58.6	79.1
Chrome	16.6	3.6	54.6	74.8
Nickel	18.4	2.6	65.2	86.2

We introduce ablation efficiency as the ratio E_{th} / E_{exp}. This ratio is dimensionless (arbitrary unit) and usually below 1. The higher the ratio is the more efficient the ablation process will be. The highest ratio value can be plotted as a function of fluence, repetition rate, pulse duration energy or dose per millimeter.

5. Results and discussion

Parameters on influence considered are fluence, repetition rate, pulse duration, energy dose per millimeter and scanning velocity.

5.1 Fluence

Fluence is one of the key parameters in laser surface processing which influences both the kinetic and the quality of ablation. In figure 2, we have plotted etch rate [$\mu m^3 \cdot pls^{-1}$] versus fluence [$J \cdot cm^{-2}$] using a logarithmic scale. As expected the etch rate grows with fluence. The slope change occurs in the range of 1 J/cm² which corresponds to the transition between the optical and the thermal regimes [1]. Etch rate decreases with increasing pulse duration. For instance, there is approximately a factor of 2 between 300 fs and 10 ps in the fluence range 0.16 to 1.3 J/cm².

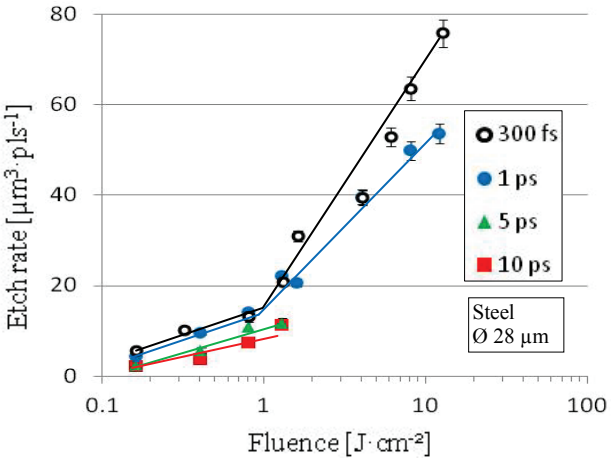

Fig. 2 Max. etch rate [$\mu m^3 \cdot pls^{-1}$] versus fluence [$J \cdot cm^{-2}$] for pulse duration ranging from 300 fs to 10 ps on a Stainless Steel target. Rep. rate used is 2 MHz up to 1.3 J/cm² then 200 kHz for higher fluencies.

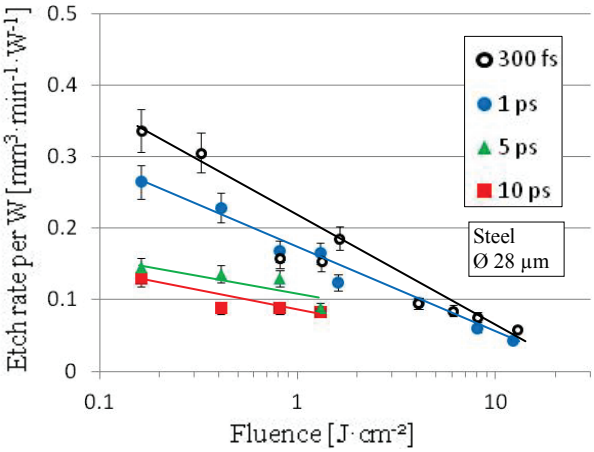

Fig. 3 Max. removal rate per average power [$mm^3 \cdot min^{-1} \cdot W^{-1}$] versus fluence [$J \cdot cm^{-2}$] for pulse duration ranging from 300 fs to 10 ps on a Stainless Steel target. Rep. rate used is 2 MHz up to 1.3 J/cm² then 200 kHz for higher fluencies.

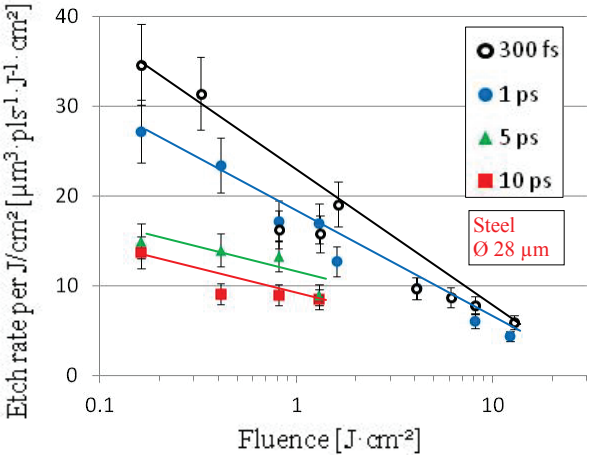

Fig. 4 Max. etch rate per fluence [$\mu m^3 \cdot pls^{-1} \cdot J^{-1} \cdot cm^2$] versus fluence [$J \cdot cm^{-2}$] for pulse duration ranging from 300 fs to 10 ps on a Stainless Steel target. Rep. rate used is 2 MHz up to 1.3 J/cm² then 200 kHz for higher fluencies.

At 12 J/cm², the removal rate is about 0.9 mm^3/min on Stainless Steel, which corresponds to 5.5µm-deep and 22µm-wide groove. The groove is engraved at 15.7 W, 200 kHz, 250 mm/s, 80 µJ/pls, with a 300fs-pulse duration. In these conditions, the ablation efficiency is 0.08 and removal rate per average power is 0.06 $mm^3 \cdot min^{-1} \cdot W^{-1}$. On the other hand, at 1.6 J/cm² the removal rate is about 0.38 mm^3/min. The average power is 2 W meanwhile both repetition rate and scanning velocities have the same values. In these operating conditions, ablation efficiency is 0.25 and removal rate per average power is 0.19 $mm^3 \cdot min^{-1} \cdot W^{-1}$. So dividing the fluence by 7.5 multiplies the ablation efficiency by 3.1.

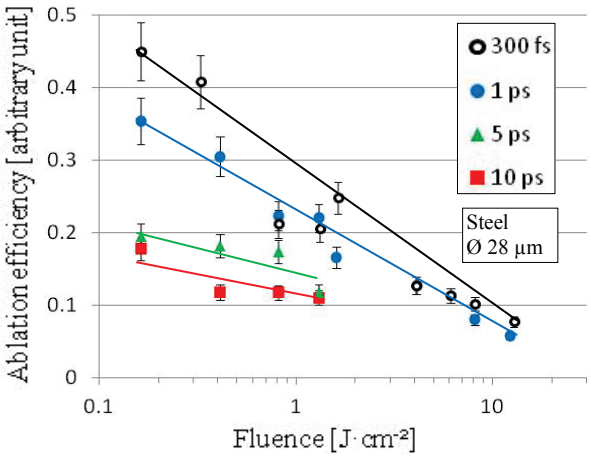

Fig. 5 Max. ablation efficiency [no unit] versus fluence [$J \cdot cm^{-2}$] for pulse duration ranging from 300 fs to 10 ps on a Stainless Steel target. Rep. rate used is 2 MHz up to 1.3 J/cm² then 200 kHz above.

Figures 3, 4 and 5 show the effect of fluence on removal rate per average power, etch rate per fluence and ablation efficiency. Using a logarithmic scale, all the curves exhibit a linear course with a negative slope. The maximum values are obtained at low fluence (0.16 J/cm²). Furthermore, the three graphs demonstrate that the efficiency of the ablation process increases significantly (x2.5 times) when the pulse duration decreases from 10 ps to 300 fs. If these graphs are displayed with a linear scale, the curves exhibit an exponential-like decay.

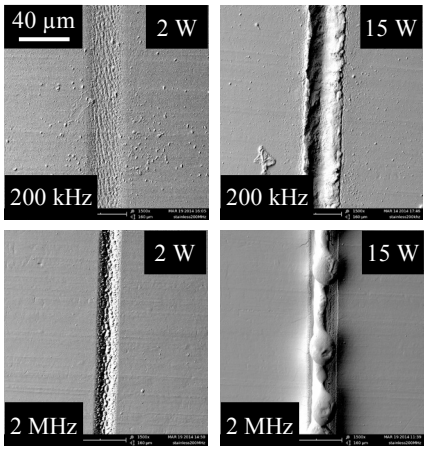

Fig. 6 SEM pictures in topography mode of a Stainless Steel foil engraved at 250 mm/s. Average power is 2 W (left) and 15 W (right). Repetition rate is 200 kHz (up) and 2 MHz (bottom). Fluence is 12.7 J/cm² (up right), 1.6 J/cm² (up left), 1.3 J/cm² (bottom right) and 0.16 J/cm² (bottom left).

According to previous results [4, 5] we expect a drop in ablation efficiency and etch rate per fluence at low fluences (below 0.16 J/cm²).

As shown in figure 6, fluence has also a significant influence on the processing quality of Stainless Steel. Indeed, burr occurrence and extend increase with fluence. For instance, at 200 kHz, rising fluence from 1.6 to 12.7 J/cm² introduces burrs and overthickness on the groove edges. Likewise, at 2 MHz, switching from 0.16 to 1.3 J/cm² turns the clean groove into a high-relief uneven track with large droplets.

Moreover, since the beam has a Gaussian spatial profile the width of the groove increases with fluence (figure 6).

Furthermore, we observe laser induced periodic surface structures (LIPSS) inside the groove at low fluence. Due to the linear polarization of the beam, these structures are perpendicular to the groove axis.

In addition, the z-profile measured using confocal microscopy at 200 kHz and 12.7 J/cm² shows two kinds of burrs in the vicinity of the groove (figure 7). These two burrs are separated by a narrow low-relief zone. The burr closest to the groove is thin and high meanwhile the other is more extended. We guess that the groove is covered by a recast layer which corresponds to the closest burr.

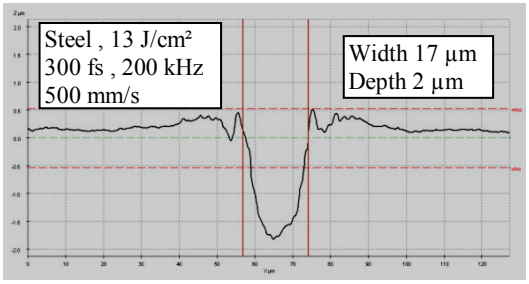

Fig. 7 Profile obtained thanks to confocal microscopy on Stainless Steel foil engraved at 500 mm/s. The width is 17µm and the depth 2 µm. Average power is 15W, rep. rate is 200 kHz and pulse duration is 300 fs.

5.2 Repetition rate

Increasing repetition from 200 kHz to 2 MHz may induce two antagonist phenomena: heat accumulation [12] on one hand and particles shielding [13] on the other hand. Heat accumulation improves the material etch rate to the detriment of the processing quality meanwhile particles shielding reduces the pulse energy available to produce ablation [10]. The effect of heat accumulation is enhanced with increasing fluences. Actually, the effect of high repetition rate on the ablation efficiency is material dependent (melting and boiling enthalpy, heat conductivity, electron-to-phonon coupling time).

On figures 8, 9 and 10 we have plotted removal rate per average power, etch rate per fluence and ablation efficiency respectively as a function of repetition rate for Stainless Steel, Aluminum, Copper and Molybdenum. The repetition rate varies from 200 kHz to 2 MHz. The pulse duration is in the range of 300 to 400 fs. We have selected the optimum values of velocity and fluence for each repetition rate level and material. For Aluminum, we notice no significant influence of repetition rate.

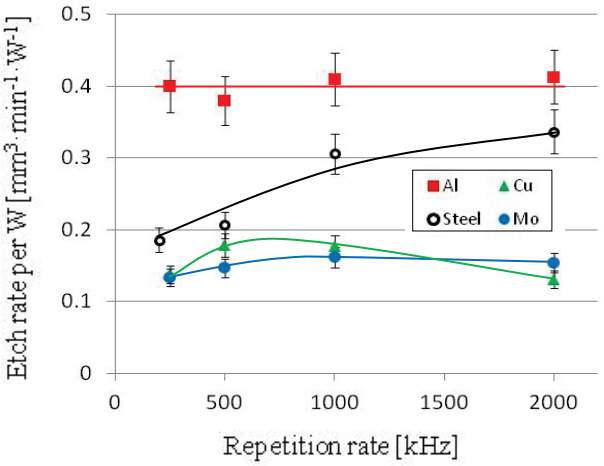

Fig. 8 Max. removal rate per average power [$mm^3 \cdot min^{-1} \cdot W^{-1}$] versus repetition rate [kHz] for Aluminum (red), Copper (green), Molybdenum (blue) and Stainless Steel (black). Pulse duration is 300-400 fs.

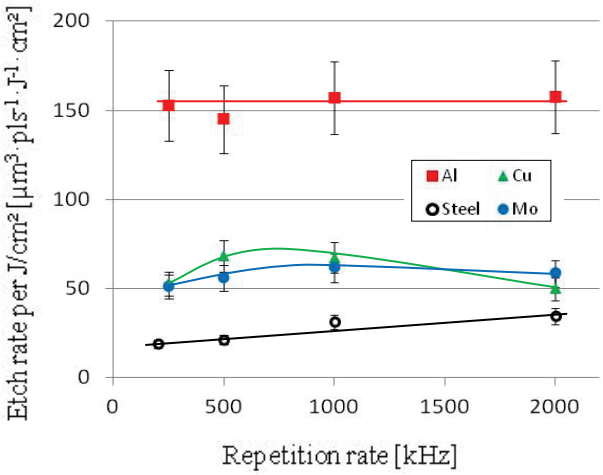

Fig. 9 Max. etch rate per fluence [$\mu m^3 \cdot pls^{-1} \cdot J^{-1} \cdot cm^2$] versus repetition rate [kHz] for Aluminum (red), Copper (green), Molybdenum (blue) and Stainless Steel (black). Pulse duration is 300-400 fs.

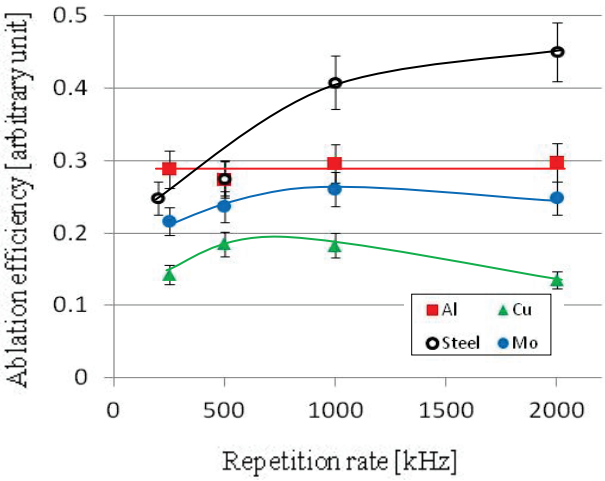

Fig. 10 Max. ablation efficiency [no unit] versus repetition rate [kHz] for Aluminum (red), Copper (green), Molybdenum (blue) and Stainless Steel (black). Pulse duration is 300-400 fs.

For Molybdenum and Copper, we see a slight effect of repetition rate on the ablation efficiency, with a maximum value in the range of 500 kHz to 1 MHz. The most significant effect is observed on Stainless Steel, since the process efficiency rises from 0.25 to 0.45 between 200 kHz and 2 MHz. We assume that this phenomenon results from heat accumulation.

Furthermore, rising repetition rate from 200 kHz to 2 MHz at high fluence while maintaining a constant scanning velocity produces some detrimental effects on the processing quality such as burr, overthickness or uncontrolled shape (see figures 6 and 11).

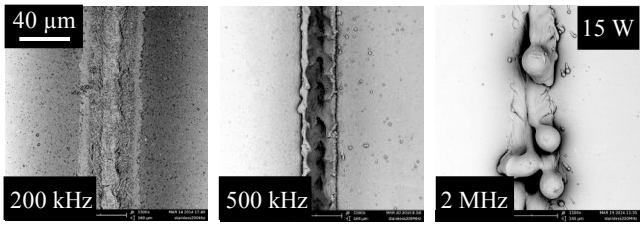

Fig. 11 SEM pictures of a Stainless Steel foil engraved at 375 mm/s with increasing rep. rate from 200 to 2000 kHz. Average power is 15W and pulse duration is about 300 to 400 fs.

5.3 Pulse duration

The evolution of removal rate per average power, etch rate per fluence and ablation efficiency versus pulse duration shown in figures 12, 13 and 14. Since repetition rate has a significant effect on Stainless Steel we have considered both kHz and MHz regimes for this material. The spot size is 28 µm for Steel and 54 µm for other metals.

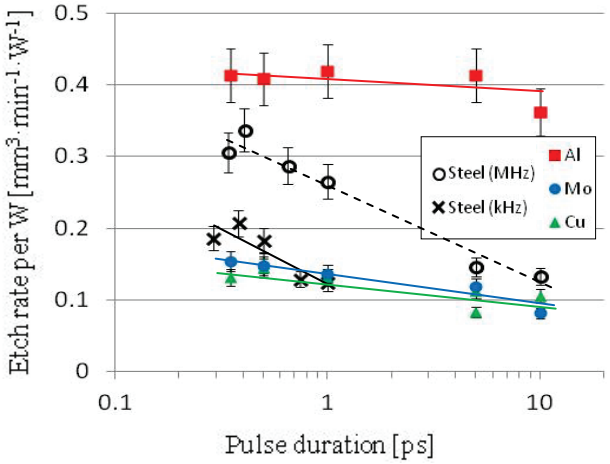

Fig. 12 Max. removal rate per average power [$mm^3 \cdot min^{-1} \cdot W^{-1}$] versus pulse duration [ps] for Aluminum (red), Copper (green), Molybdenum (blue) and Stainless Steel (black, hollow dot for MHz regime, cross for kHz regime).

The influence of pulse duration on ablation efficiency is highly material-dependent (figure 14). Indeed, we observe no significant effect on Aluminum (variation is smaller than uncertainty), a slight effect on Copper (-25%), and a major effect on Molybdenum (-50%) and on Stainless Steel (-60%) when the pulse duration is risen from 300 fs to 10 ps. This tendency confirms results previously published by Ancona [10] and Neuenschwander [11].

Moreover, removal rate per average power values obtained on Copper and Stainless Steel at 10 ps (figure 10) are consistent with respect to those published by Lauer [15] and Jaeggi [16], although the experimental protocol is quite different (measures are done on dots or squares, not lines). In addition, we notice that etch rate and etch rate per fluence on Aluminum is 3 to 6 times higher than on other metals on a wide process window (figure 13).

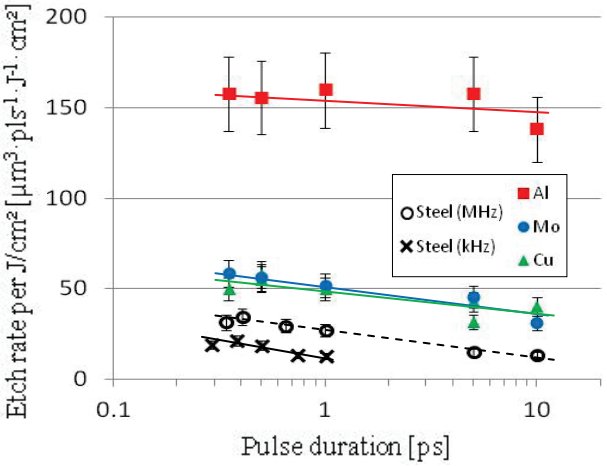

Fig. 13 Max. etch rate per fluence [$\mu m^3 \cdot pls^{-1} \cdot J^{-1} \cdot cm^2$] versus pulse duration [ps] Aluminum (red), Copper (green), Molybdenum (blue) and Stainless Steel (black, hollow dot for MHz regime, full dot for kHz regime).

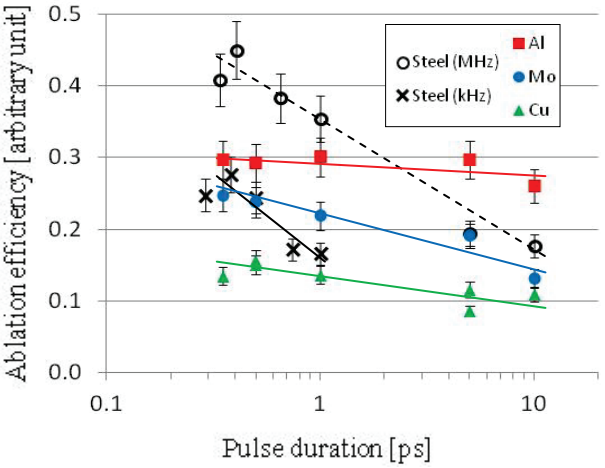

Fig. 14 Max. ablation efficiency [no unit] versus pulse duration [ps] Aluminum (red), Copper (green), Molybdenum (blue) and Stainless Steel (black, hollow dot for MHz regime, full dot for kHz regime).

5.4 Dose per millimeter

Dose per millimeter is calculated using the following formula: Dose=Rep.Rate*Energy/Velocity. The unit is [$J \cdot mm^{-1}$]. In figure 15, we have plotted etch rate per fluence as a function of dose for a 300fs-pulse duration. We observe four different behaviors between Stainless Steel, Aluminum, Copper and Molybdenum. Indeed, due to its

high thermo-physical properties, Molybdenum can stand a high dose or thermal load (up to 0.4 J·mm^{-1}) meanwhile Aluminum and Stainless Steel give burr and melting at low dose (below 0.1 J·mm^{-1}). Copper exhibits an intermediate behavior.

So, for each material we can define a critical dose beyond which there is a drastic drop in etch rate per fluence, and a maximum dose beyond which the groove collapses due to melting and there is no engraving anymore. The experimental values of critical and maximum doses are shown in table 2.

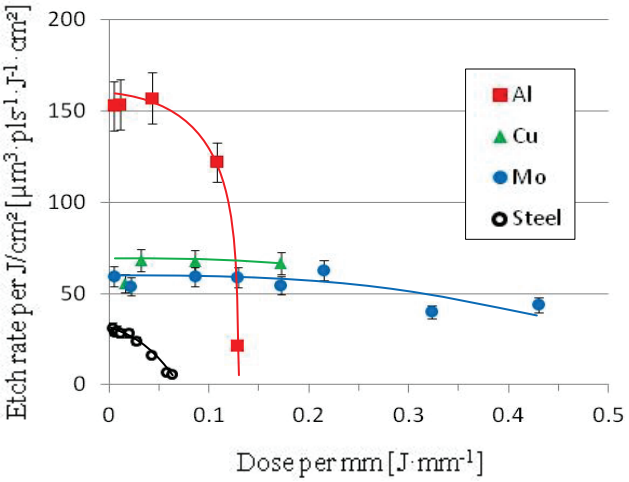

Fig. 15 Max. etch rate per fluence [µm^3·pls^{-1}·J^{-1}·cm^2] versus dose per mm [J·mm^{-2}] at 300 fs for Aluminum, Stainless Steel, Copper and Molybdenum. Spot size is 28 µm.

Table 2 Critical and maximum doses for Stainless Steel, Aluminum, Copper and Molybdenum

Material	Critical dose [J·mm^{-1}]	Max. dose [J·mm^{-1}]
Stainless Steel	0.02	0.06
Aluminum	0.08	0.13
Copper	0.22	0.22
Molybdenum	0.22	0.43

Therefore, the figure 15 can be used as an abacus. It is possible to maintain a good processing quality and process efficiency as long as the actual dose is below the critical dose. Above the critical dose, a significant part of the incoming pulse energy will be spent in thermal effects and will be not available to produce ablation, so the process will be less efficient. Likewise, the feasibility of engraving is guaranteed as long as the actual dose is below the maximum dose.

Furthermore, for a given repetition rate and a given pulse energy, the minimum scanning velocity required to engrave a groove can be calculated from the formula: $V_{min.}$=Rep.Rate*Energy/Maximum Dose. For instance, at 15W and 200 kHz, the minimum velocity is 250 mm/s. This value can be correlated to SEM observations as shown in paragraph 5.5.

Moreover, in figure 16 we have plotted etch rate per fluence as a function of dose for different pulse durations ranging from 300 fs to 10 ps on a Stainless Steel target. We observe a significant decrease in etch rate per fluence as the pulse duration increases. However the maximum dose remains constant with pulse duration in the investigated range.

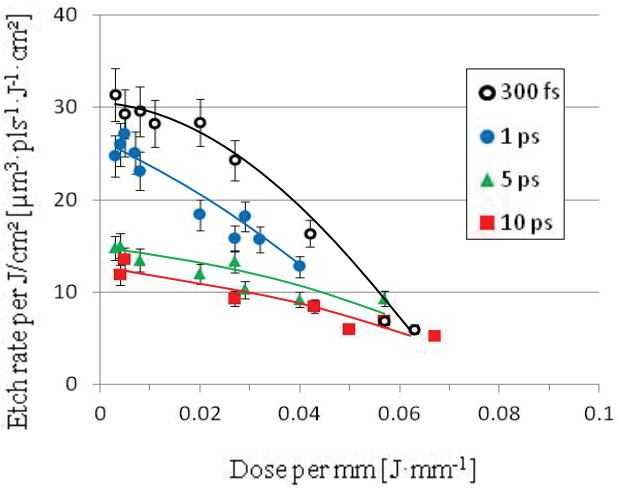

Fig. 16 Max. etch rate per fluence [µm^3·pls^{-1}·J^{-1}·cm^2] versus dose per mm [J·mm^{-2}] at 300 fs (black), 1 ps (blue), 5 ps (green) or 10 ps (red) for a steel target. Spot size is 28 µm.

5.5 Scanning velocity

The thermal load deposited into the target material increases with decreasing scanning velocity as it is shown in figures 17 (full mode SEM) and 18 (topography mode SEM, samples engraved at 15 W). If the actual velocity is higher than the minimum velocity defined by the maximum dose (250 mm/s), then it is possible to maintain a good ablation efficiency (see table 3). When the actual velocity becomes smaller than the minimum velocity, melting will occur inside and in the vicinity of the groove. Then extensive burrs, droplets and roughness will appear. It is not even possible to measure the ablated volume accurately.

If the velocity keeps on decreasing then the groove will collapse and it's not engraving anymore. Similar behavior on Molybdenum has been reported in a previous paper [5].

Furthermore, as shown in figure 18, the scanning velocity has a major effect on processing quality at high fluence (13 J/cm², 15 W at 200 kHz), but has less effect at low fluence (1.6 J/cm², 2 W at 200 kHz). As explained in paragraph 5.1, working at low fluence enables to avoid burr, overthickness and droplet appearance.

So, the best process efficiency and processing quality are obtained at low fluence. Therefore, scaling up from 2 W to 15 W implies to work with high repetition rate and very high deflection speed (in order to overbalance heat accumulation produced by high repetition rate). In these conditions, producing deep grooves will require several passes.

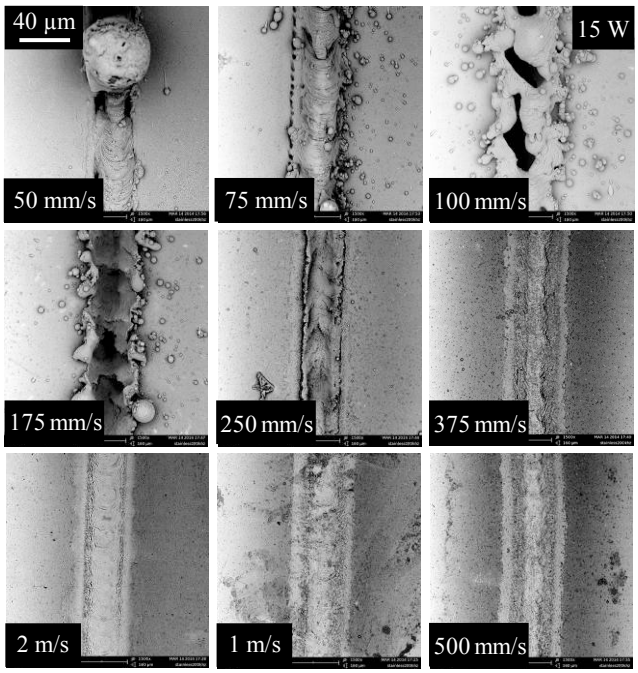

Fig. 17 SEM pictures of a Stainless Steel foil engraved with scanning velocities ranging from 50 mm/s to 2 m/s. Average power is 15W, rep. rate is 200 kHz and pulse duration is 300 fs.

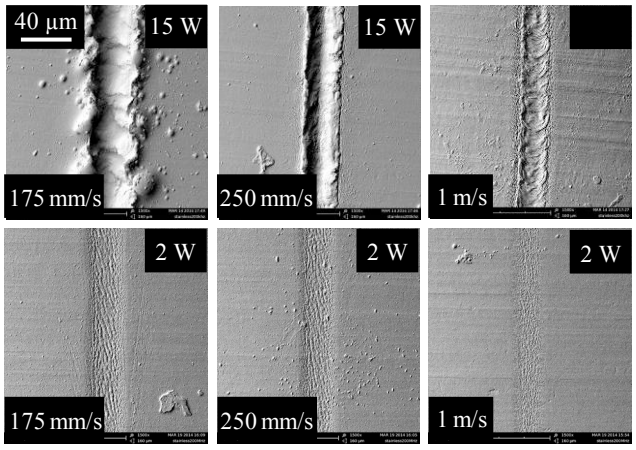

Fig. 18 SEM pictures in topography mode of a Stainless Steel foil engraved at 175, 250 and 1000 m/s. Rep. rate is 200 kHz and pulse duration is 300 fs. Average power is 15 W (up) and 2 W (bottom)

Table 3 Dose and removal rate per average power for a given scanning velocity on Stainless Steel at 300 fs, 200 kHz and 15 W. The red frame indicates the maximum dose and the minimum velocity.

Velocity [mm·s^{-1}]	Dose per mm [J·mm^{-1}]	Rem. rate per W [mm^3·min^{-1}·W^{-1}]
1000	0.015	0.053
500	0.03	0.058
375	0,04	0.054
250	0,06	0.058
175	0.09	-

6. How long to remove 1 mm3 of Stainless Steel?

From a practical point of view what could be the processing time to remove 1 mm^3 of Stainless Steel with an ultrashort laser? Table 4 and 5 show the time to remove 1 mm^3 of Stainless Steel at 15 and 2 Watt respectively. Corresponding SEM pictures are regrouped in figure 19. We compare 200 kHz to 2 MHz at 300-400 fs, and 400 fs to 10 ps at 2 MHz.

The shorter processing time are obtained in the MHz-regime at 400 fs: 24 seconds at 15 W and 89 seconds at 2 W. The ablation efficiency is 0.21 and 0.45 respectively.

In addition, the best processing quality is clearly obtained at 2 W, that is to say 1.6 J/cm² at 200 kHz or 0.16 J/cm² at 2 MHz (see figure 19). In both cases there is neither burr nor droplet.

Table 4 Time required to remove 1 mm^3 of Stainless Steel at 15 W, 200kHz-2MHz comparison and 400fs-10ps comparison

Pulse duration / Repetition rate	300fs 200kHz	400fs 2MHz	10ps 2MHz
Velocity [mm/s]	250	500	375
Fluence [J/cm²]	13	1.3	1.3
Removal rate [mm^3/min]	0.9	2.5	1.3
Ablation efficiency	0.08	0.21	0.11
Time to ablate 1mm^3	66s	24s	45s

Table 5 Time required to remove 1 mm^3 of Stainless Steel at 2 W, 200kHz-2MHz comparison and 400fs-10ps comparison

Pulse duration / Repetition rate	300fs 200kHz	400fs 2MHz	10ps 2MHz
Velocity [mm/s]	250	2000	2000
Fluence [J/cm²]	1.6	0.16	0.16
Removal rate [mm^3/min]	0.37	0.68	0.23
Ablation efficiency	0.25	0.45	0.15
Time to ablate 1mm^3	162s	89s	260s

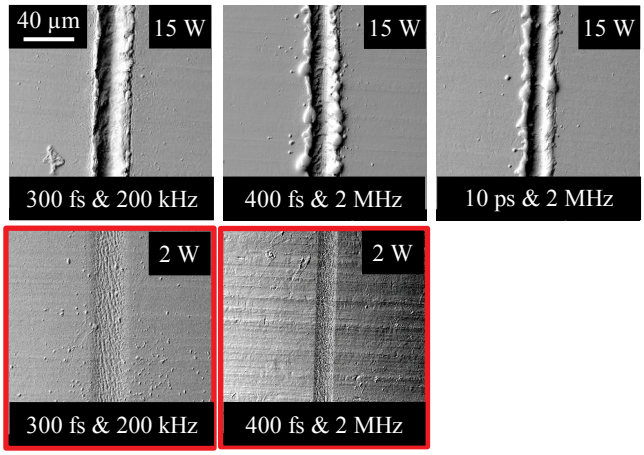

Fig. 19 SEM pictures in topography mode of a Stainless Steel foil engraved 300 fs & 200 kHz (left), 400 fs & 2 MHz (middle), and 400 fs & 2 MHz (right). Average power is 15 W (up) and 2 W (bottom). No picture at 2W & 10 ps

7. Conclusion

In this paper we have shown that it is possible to produce surface ablation of Stainless Steel with a high power ultrashort pulses laser (up to 15 W) operating in both kHz and MHz regimes.

The results obtained on Stainless Steel were compared to those previously published on Aluminum, Copper and Molybdenum. It appears that the effect of pulse duration, repetition rate, energy dose per mm and scanning velocity is highly material dependent. Ablation efficiency on Stainless Steel is quite sensitive to these parameters, so the process windows are narrower compared to other metals. Moreover, for each material there is an energy dose beyond which the groove collapses due to melting. This dose value can be determined experimentally and correlated to SEM observations.

The best process efficiency and processing quality (burr-free) on Stainless Steel are obtained at low fluence and with femtosecond pulses. So, scaling up from 2 W to 15 W implies to work with high repetition rate and very high deflection speed (over 10 m/s). In these conditions, producing deep grooves will require several passes.

Acknowledgments and Appendixes

We acknowledge the European Commission, the French Ministry of Research and the Aquitaine Regional Council for support and funding. We also thank Beat Neuenschwander and Beat Jaeggi from the Bern University of Applied Sciences for scientific interactions.

References

[1] Chichkov, B. N., Momma, C., Nolte, S., Von Alvensleben, F. and Tünnermann, A., Femtosecond, picosecond and nanosecond laser ablation of solids, Appl. Phys. A, 63, 109-115 (1996)

[2] Momma, C., Chichkov, B., N., Nolte, S., Von Alvensleben, F., Tünnermann, A., Welling, H. & Wellegehausen, B., Short-pulse laser ablation of solid targets, Opt. Com., 129, 134-142 (1996)

[3] Shah, L., Fermann, M., Dawson, J. & Barty, P., Micromachining with a 50W, 50µJ, subpicosecond fiber laser system, Opt. Express, 14, 25, 12546-12551 (2006)

[4] Lopez, J., Torres, R., Zaouter, Y., Georges, P., Hanna, M., Mottay, E. and Kling, R., Study on the influence of repetition rate and pulse duration on ablation efficiency using a new generation of high power Ytterbium doped fiber ultrafast laser, in Proceedings of SPIE, Vol. 8611, 861118-1 (2013)

[5] Lopez, J., Zaouter, Y., Torres, R., Faucon, M., Hönninger, C., Georges, P., Hanna, M., Mottay, E. and Kling, Parameters of influence in surface ablation of metals with using a high power tunable ultrafast laser, in Proceedings of the International Congress on Applications of Laser & Electro-Optics, M303, 686-694 (2013)

[6] Wellershoff, S.-S., Hohlfeld, J., Güdde, J. and Matthias, E., The role of electron-phonon coupling in femtosecond laser damage of metals, Appl. Phys. A, Vol. 69, S99-S107 (1999)

[7] Byskov-Nielsen, J., Savolainen, J.-M., Christensen, M. S. and Balling, P., Ultra-short pulse laser ablation of copper, silver and tungsten: experimental data and two-temperature model simulations, Appl. Phys. A, Vol. 103, 447-453 (2011)

[8] Anisimov, S. I. and Lukyanchuk, B. S., Selected problems of laser ablation theory", Vol. 45, 293-324 (2002)

[9] Le Harzic, R., Breitling, D., Weikert, M;, Sommer, S., Föhl, C., Valette, S., Donnet, C., Audouard, E. and Dausinger, F., Pulse width and energy influence on laser micromachining of metals in a range of 100fs to 5 ps, Appl. Surf. Sci., Vol. 249, 322-331 (2005)

[10] Ancona, A., Döring, S., Jauregui, C., Röser, F., Limpert, J., Nolte, S. & A. Tünnermann, A., Femtosecond and picosecond laser drilling of metals at high repetition rates and average powers, Opt. Lett. 34, 3304-3306 (2009)

[11] Neuenschwander, B., Jaeggi, B. and Schmid, M., From ps to fs : dependence of the material removal rate and the surface quality on the pulse duration for metals, semiconductors and oxides, in Proceedings of the International Congress on Applications of Laser & Electro-Optics, M1004, 959-968 (2012)

[12] Vorobyev, A.Y. and Guo, C., Direct observation of enhanced residual thermal energy coupling to solids in femtosecond laser ablation, Appli. Phys. Lett., Vol. 86, 011916 (2005)

[13] König, J., Nolte, S. and Tünnermann, A., Plasma evolution during metal ablation with ultrashort pulses, Opt. Express, Vol. 13, 10597-10607 (2005)

[14] Neuenschwander, B., Jaeggi, B. and Schmid, M.,From fs to sub-ns : dependence of the material removal rate on the pulse duration on metals, Phys. Proc., Vol. 41, 794-801 (2013)

[15] Lauer, B., Neuenschwander, B., Jaeggi, B. and Schmid, M., From fs-ns : Influence of the pulse duration onto the material removal rate and machining quality for metals, in Proceedings of the International Congress on Applications of Laser & Electro-Optics, paper M309 (2013)

[16] Jaeggi, B., Neuenschwander, B., Zimmermann, M., Penning, L., deLoor, R. , Weingarten, K. and Oehler, A., High throughout and high precision laser micromachining with ps-pulses in synchronized mode with a fast polygon line scanner, in Proceedings of SPIE Photonics West, Vol 8967, paper 25 (2014)

[17] Chase, M.W., Jr., NIST-JANAF Thermochemical Tables, Fourth Edition, J. Phys. Chem. Ref. Data, Monograph 9, 1-1951 (1998)

(Received: March 31, 2014, Accepted: July 28, 2014)